Macromolecules

NOTE

pubs.acs.org/Macromolecules

Hairy Hybrid Microrattles of Metal Nanocore with Functional Polymer Shell and Brushes

Guo Liang Li, Li Qun Xu, K. G. Neoh, and E. T. Kang*

Department of Chemical & Biomolecular Engineering, National University of Singapore, Kent Ridge, Singapore 119260

Supporting Information

INTRODUCTION

Hollow micro- and nanospheres have received considerable attention because of their relevant applications as drug encapsulates, as transducers and dielectrics for electronics, and as capsules for catalytic reactions and hydrogen storage.[1−7] A variety of chemical and physicochemical approaches, such as hard and soft template approaches, self-assembly of block copolymers, and template-free synthesis, have been developed to produce inorganic, polymer, and hybrid hollow particles.[8−13] Among the various approaches reported so far, template-directed synthesis is probably the most widely used method for the generation of hollow particles with precisely controlled size and shell thickness. The process generally involves the removal of either the hard template core by chemical dissolution[9,13] or soft template core by thermal decomposition from the core−shell precursors.[10] Moreover, regulation of morphology, surface functionality, size, and size distribution of these hollow micro- or nanospheres is always required to improve their performance in practical applications, such as in drug delivery systems (DDS).[4]

It is highly desirable to functionalize the polymer hollow microspheres through postmodification of interior void space and/or exterior shell surfaces. On one hand, functionalization of the interior void space can be achieved by encapsulation of guest species.[14−17] Inorganic hollow particles encapsulating a movable metal core in the hollow cavity, termed the "yolk−shell" or "rattle-type" structure, have been widely reported.[18−21] In addition to the well-defined hollow structures, rattle-type inorganic particles also exhibit improved/enhanced activity in catalytic reactions[20] and can serve as contrast agents in magnetic resonance imaging (MRI).[21] On the other hand, exterior surface modification via the thiol−ene click chemistry is highly efficient, free of byproduct, and does not require toxic transition metals as catalyst.[22−34] The thiol−ene click chemistry has recently been explored for the construction of novel macromolecular architectures and for "click" functionalization of silicon substrate,[30] polymer nanoparticles,[31,32] and protein-immobilized biochips.[33,34]

In this paper, we describe a synthesis route to hairy rattle-type hybrid microspheres consisting of a metal nanocore (gold or silver), a poly(methacrylic acid-*co*-divinylbenzene) (P(MAA-*co*-DVB)) shell, and functional polymer brushes clicked on the exterior surface. The incorporation of metal nanocore was achieved by using the gold@silica or silver@silica core−shell nanoparticles as templates for the formation of metal@silica@polymer core−double shell microspheres. The thiol-terminated polymer chains of hydrophilic poly(ethylene glycol) (PEG-SH) or thermoresponsive poly(*N*-isopropylacylamide) (PNIPAM-SH) were covalently grafted onto the residual double bonds of the DVB unit on the microsphere surface via the thiol−ene "click" reaction to produce a hairy surface of tailored functionality. The application of bifunctional hollow microspheres for the confined heterogeneous catalytic reaction was also demonstrated.

Scheme 1. Schematic Illustration of the Synthesis of Hairy Metal@Air@Polymer Hybrid Microrattles with a Metal Nanocore, a Cross-Linked Polymer Shell, and Functional Polymers Brushes on the Exterior Surface[a]

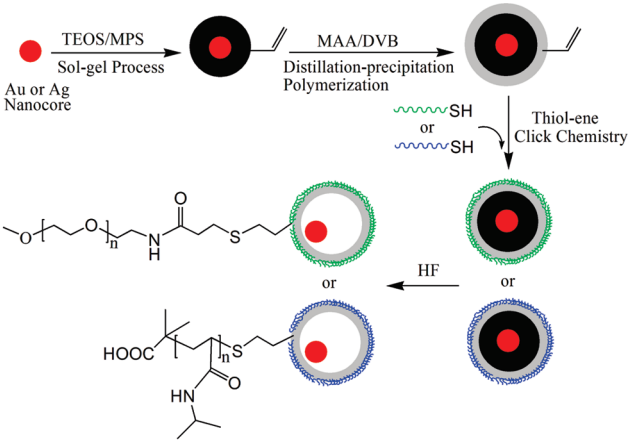

[a] PEG = poly(ethylene glycol); PNIPAM = poly(*N*-isopropylacrylamide).

RESULTS AND DISCUSSION

Procedures for the synthesis of hairy hybrid microrattles, consisting of a metal (gold or silver) nanocore, a cross-linked polymer shell, and functional polymer brushes on the exterior surface, from the hairy core−double shell microspheres are shown in Scheme 1. Initially, Au@SiO_2-MPS and Ag@SiO_2-MPS core−shell templates with C═C double bonds on the surface were prepared via coating of a silica shell on the metal (Au or Ag) nanocores in the sol−gel reaction of tetraethyl orthosilicate

Received: January 15, 2011
Revised: February 21, 2011
Published: March 14, 2011

Table 1. Size, Size Distribution, and Shell Thickness of the Metal@Silica Core−Shell and Metal@Silica@Polymer Core−Double Shell Microspheres

sample	D_n[a] (nm)	D_w[a] (nm)	PDI[a]	shell thickness[b] (nm)	CV[a] (%)
Au nanocore-1	18	19	1.09		21
Au nanocore-2	23	23	1.03		19
Au nanocore-3	45	47	1.04		18
Ag nanocore	38	56	1.48		39
Au@SiO_2-MPS core−shell-1[c]	135	139	1.03	59	13
Au@SiO_2-MPS core−shell-2[c]	157	168	1.07	70	15
Au@SiO_2-MPS core−shell-3[c]	196	207	1.06	90	9
Ag@SiO_2-MPS core−shell	70	73	1.05	16	13
Au@SiO_2@P(MAA-*co*-DVB) core−double shell[d]	308	315	1.02	56	11
Ag@SiO_2@P(MAA-*co*-DVB) core−double shell	160	169	1.06	45	15

[a] D_n is the number-average diameter, D_w is the weight-average diameter, PDI is the polydispersity index, and CV is the coefficient of variation (see Experimental Section, Supporting Information). [b] The shell thickness of the core−shell and core−double shell was determined from the TEM images. [c] The Au@SiO_2-MPS core−shell microspheres were prepared using the Au nanocore-1 as seeds. [d] Au@SiO_2@P(MAA-*co*-DVB) core−double shell microspheres were prepared using the Au@SiO_2-MPS core−shell-3 as seeds.

(TEOS) and 3-(trimethoxysilyl)propyl methacrylate (MPS).[35,36] Subsequently, distillation−precipitation polymerization of methacrylic acid (MAA), in the presence of divinylbenzene (DVB, a cross-linking agent), from the Au@SiO_2-MPS (or Ag@SiO_2-MPS) core−shell nanoparticle (NP) templates produces the Au@SiO_2@P(MAA-*co*-DVB) (or Ag@SiO_2@P(MAA-*co*-DVB)) core−double shell microspheres with residual C═C double bonds from the DVB units on the surface.[37,38] The thiol-terminated poly(ethylene glycol) (PEG-SH) or poly(*N*-isopropylacrylamide) (PNIPAM-SH) chains are grafted onto the surface of Au@SiO_2@P(MAA-*co*-DVB) core−double shell microspheres via the surface thiol−ene "click" reaction. Finally, the hairy Au@air@P(MAA-*co*-DVB)-*click*-PEG (or Ag@air@P(MAA-*co*-DVB)-*click*-PNIPAM) hybrid microrattles consisting of a gold (or silver) nanocore, cross-linked poly(MAA-*co*-DVB) polymer shell, and functional PEG (or PNIPAM) brushes on the exterior surfaces are obtained through selective removal of the silica inner shell by HF etching of the hairy Au@SiO_2@P(MAA-*co*-DVB)-*click*-PEG (or Ag@SiO_2@P(MAA-*co*-DVB)-*click*-PNIPAM) core−double shell microspheres.

Gold NPs of 18, 23, and 45 nm in diameter were synthesized, a priori, via the standard sodium citrate reduction method (Table 1 and Figure S1, Supporting Information), by tuning the molar ratio of sodium citrate to hydrogen tetrachloroaurate trihydrate (gold precursor) from 2:1 to 1.5:1 to 1:1, respectively. Figure 1a shows the transmission electron microscopy (TEM) image of the synthesized Au NPs with an average diameter of 18 nm. The thickness of subsequent silica coating can be controlled by varying the TEOS precursor concentration in the sol−gel reaction (Experimental Section, Supporting Information). The TEM images of 135 and 196 nm Au@SiO_2-MPS core−shell nanospheres with the corresponding silica shell thicknesses of 59 and 90 nm are shown in parts b and c of Figure 1, respectively. Well-defined core−shell NPs with uniform surfaces are observed in these TEM images. The size, size distribution, and shell thickness of as-synthesized Au@SiO_2-MPS core−shell nanospheres are summarized in Table 1. The Fourier-transform infrared (FT-IR) spectrum of Au@SiO_2-MPS core−shell nanospheres (Figure S2, Supporting Information) reveals an absorption peak at 1632 cm^{-1}, associated with the C═C group from MPS on the surface of Au@SiO_2-MPS core−shell template NPs.

Distillation−precipitation polymerization has recently been explored for the synthesis of well-defined silica@polymer core−shell and hierarchical hollow polymer structures for drug delivery systems (DDS).[39] In this work, distillation−precipitation polymerization of MAA was carried out in the presence of DVB in acetonitrile, using the Au@SiO_2-MPS core−shell-3 NPs of Table 1 as templates, to produce the core−double shell microspheres with a cross-linked P(MAA-*co*-DVB) outer shell. The PEG-thiol chains (PEG-SH, M_n 5000 g/mol) were subsequently grafted to the exterior surface of the Au@SiO_2@P(MAA-*co*-DVB) core−double shell microspheres via the surface thiol−ene "click" reaction (Scheme 1). The field-emission scanning electron microscopy (FESEM) image of the as-prepared Au@SiO_2@P(MAA-*co*-DVB) core−double shell microspheres of 308 nm in average size is shown in Figure 1d. The microspheres retain the spherical structure after the formation of a cross-linked polymer outer shell on the Au@SiO_2-MPS core−shell NPs. The TEM image (inset of Figure 1d) of the synthesized Au@SiO_2@P(MAA-*co*-DVB) microspheres reveals an outer polymer shell of low contrast encapsulating a dense Au@SiO_2 inorganic core−shell particle. The cross-linked poly(MAA-*co*-DVB) outer shell of the core−double shell microspheres is about 56 nm in thickness. In addition to providing a cross-linked, stable (resistant to acid, base, and organic solvent) and rigid polymer outer shell, the PDVB segments also provide residual C═C double bonds on the exterior surface of the Au@SiO_2@P(MAA-*co*-DVB) microspheres.[37,38,40] The FT-IR spectrum of the Au@SiO_2@P(MAA-*co*-DVB) core−double shell microspheres shows an absorption peak at 1632 cm^{-1} (Figure S3a, Supporting Information), confirming the persistence of vinyl groups from PDVB segments on the microsphere surfaces. These C═C groups will serve as active sites for the "click" reaction with thiol-terminated polymer chains to produce the hairy functional microspheres.

Poly(ethylene glycol) (PEG) and its derivatives have been widely used in biomedical and biomaterials applications.[41−43] The PEG chains with thiol-terminal groups were first characterized by X-ray photoelectron spectroscopy, or XPS (Figure S4, Supporting Information), and were used to modify the exterior surface of Au@SiO_2@P(MAA-*co*-DVB) core−double shell microspheres via the surface thiol−ene "click" reaction. Figure 2a,b shows the respective wide-scan and C 1s core-level spectra of the Au@SiO_2@P(MAA-*co*-DVB) microspheres prior to click grafting

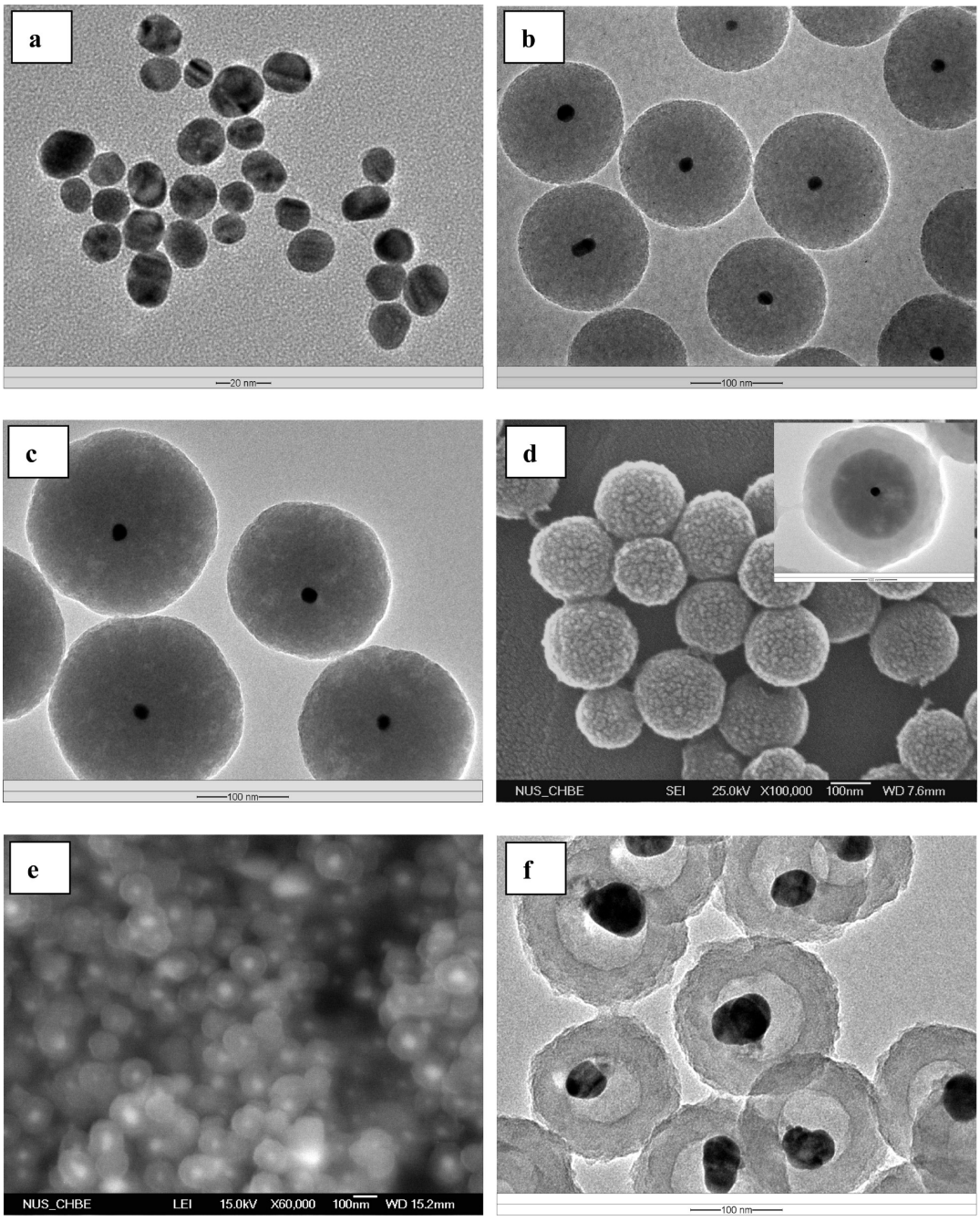

Figure 1. TEM and FESEM micrographs of the (a) 18 nm gold (Au) nanocores, (b) 135 nm Au@SiO_2-MPS, and (c) 196 nm Au@SiO_2-MPS core−shell microspheres, (d) 308 nm Au@SiO_2@P(MAA-*co*-DVB) core−double shell microspheres, and (e, f) Ag@air@P(MAA-*co*-DVB)-*click*-PNIPAM hybrid microrattles (MPS: 3-(trimethoxysilyl)propyl methacrylate; MAA: methacrylic acid; DVB: divinylbenzene; PNIPAM: poly(*N*-isopropylacrylamide)). The scale bars for (a−f) are 20, 100, 100, 100, 100, and 100 nm, respectively.

of the PEG brushes. The XPS C 1s core-level spectrum in Figure 2b shows predominantly two peak components having binding energies (BEs) at 284.6 and 288.8 eV, attributable to the C−C/C−H and O═C−O species, respectively, of the cross-linked P(MAA-*co*-DVB) outer shell of the microspheres.[44] After grafting of the PEG brushes via the surface click reaction, the XPS wide-scan spectrum of the Au@SiO_2@P(MAA-*co*-DVB)-*click*-PEG microspheres in Figure 2c shows an increase in the relative intensity of O 1s signal. The XPS C 1s core-level spectrum of the microspheres (Figure 2d) can be curved-fitted with three peak components having BEs at about 284.6, 286.1, and 288.8 eV, attributable to the C−C/C−H, C−O/C−S, and O═C−O species, respectively.[45] The C−O/C−S species are associated with the grafted PEG brushes on the exterior surface of the microspheres. The FT-IR absorption bands of the Au@SiO_2@P-(MAA-*co*-DVB)-*click*-PEG microspheres at 1164 and 1380 cm^{-1} are associated respectively with the vibration of C−O and $-CH_3$ groups from the grafted PEG brushes on the exterior surface of microspheres (Figure S3b, Supporting Information). The silica inner shell in the Au@SiO_2@P(MAA-*co*-DVB)-*click*-PEG

dx.doi.org/10.1021/ma200102n |*Macromolecules* 2011, 44, 2365–2370

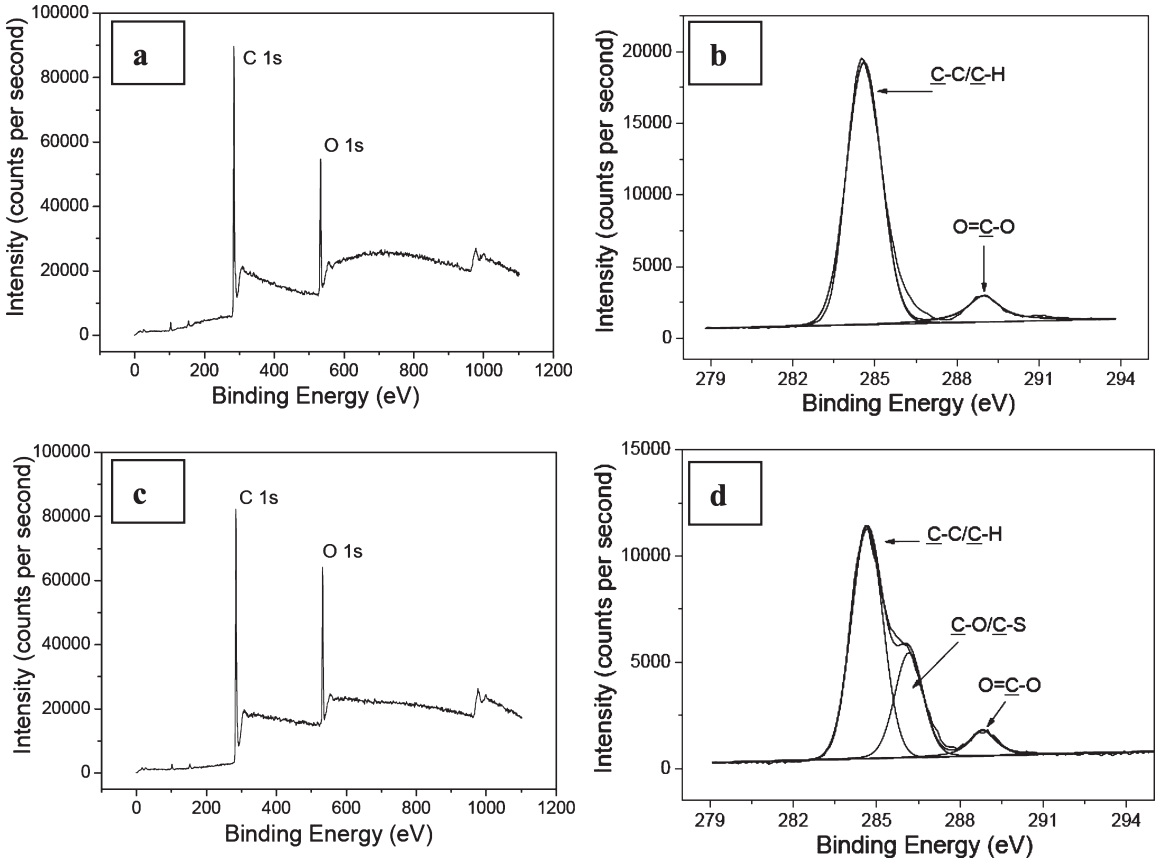

Figure 2. XPS wide-scan and C 1s core-level spectra of the (a, b) Au@SiO_2@P(MAA-*co*-DVB) and (c, d) Au@SiO_2@P(MAA-*co*-DVB)-*click*-PEG (MAA: methacrylic acid; DVB: divinylbenzene; PEG: poly(ethylene glycol)).

core−double shell microspheres serves as the sacrificial materials in the production of Au@air@P(MAA-*co*-DVB)-*click*-PEG rattle-type hollow structures, as shown in Scheme 1.

Silica can be readily coated on many colloidal particles via sol−gel reaction to from core−shell nanostructures.[46] Well-defined Ag nanocore, Ag@SiO_2-MPS core−shell NPs, Ag@SiO_2@P(MAA-*co*-DVB) core−double shell, and Ag@SiO_2@P(MAA-*co*-DVB)-*click*-PNIPAM hairy core−double shell microspheres, as well as the corresponding Ag@air@P(MAA-*co*-DVB)-*click*-PNIPAM hairy hybrid microrattles, were also synthesized in the present work to illustrate the versatility of the approach to hollow polymer microspheres with different kinds of metal nanocore in the void space and polymer brushes on the exterior surface. The respective TEM images of the 38 nm Ag nanocores, 70 nm Ag@SiO_2-MPS core−shell NPs, and 160 nm Ag@SiO_2@P(MAA-*co*-DVB) core−double shell microspheres are shown in Figure S5 (Supporting Information). For the modification of exterior surfaces via the thiol−ene coupling reaction, thermoresponsive PNIPAM-SH chains with a molecular weight of 11 600 g/mol and polydispersity index (PDI) of 1.32 (from GPC analysis, Figure S6, Supporting Information) were grafted to the outer shell of the Ag@SiO_2@P(MAA-*co*-DVB) microspheres to produce the hairy Ag@SiO_2@P(MAA-*co*-DVB)-*click*-PNIPAM core−double shell microspheres. The XPS wide-scan and C 1s core-level spectra (Figure S7, Supporting Information) and the FT-IR absorption spectra (Figure S8, Supporting Information) of the microspheres before and after click reaction further confirm the grafting of PNIPAM brushes on the Ag@SiO_2@P(MAA-*co*-DVB) core−double shell microspheres surface. The XPS wide scan spectrum of the Ag@SiO_2@P(MAA-*co*-DVB)-*click*-PNIPAM core−double shell microspheres shows a new peak component with BE at about 400 eV, attributable to the N 1s species (inset of Figure S7) from the grafted PNIPAM brushes on the exterior surface. The FT-IR spectrum of hairy Ag@SiO_2@P(MAA-*co*-DVB)-*click*-PNIPAM core−double shell microspheres exhibit two new absorption peaks at 1648 cm^{-1} (amide I mode of C═O) and 1550 cm^{-1} (amide II mode of N−C═O), which are characteristic of the stretching vibration of the amide groups from PNIPAM brushes.[47] The vinyl absorption band at 1632 cm^{-1} from the PDVB segments has disappeared completely after the thiol−ene click reaction.

The thermoresponsive behavior of the grafted PNIPAM brushes on the exterior surface of core−double shell microspheres was characterized by dynamic light scattering (DLS) measurements. The hydrodynamic diameter (D_h) of hairy Ag@SiO_2@P(MAA-*co*-DVB)-*click*-PNIPAM core−double shell microspheres decreases from 258 to 212 nm as the temperature of the aqueous medium increases from 25 to 50 °C (Figure S9, Supporting Information). This phenomenon is due to the fact that PNIPAM exhibits a lower critical solution temperature (LCST) of 32 °C in an aqueous solution.[30,48] When the temperature of medium is higher than LCST, the grafted PNIPAM brushes on the exterior surface of the core−double shell microspheres associate hydrophobically, leading to the decrease in hydrodynamic size of the Ag@SiO_2@P(MAA-*co*-DVB)-*click*-PNIPAM microspheres. Hairy Ag@air@P(MAA-*co*-DVB)-*click*-PNIPAM hybrid microrattles

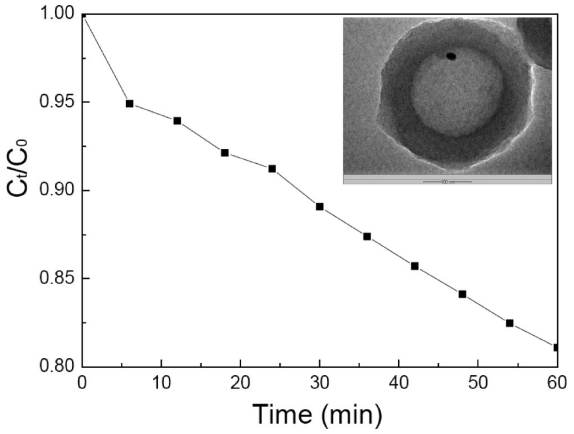

Figure 3. Catalytic reduction of *p*-nitrophenol in the cavity of Au@air@P(MAA-*co*-DVB)-*click*-PEG hybrid microrattles (C_0 and C_t are the initial and instantaneous concentrations of *p*-nitrophenol, respectively, $C_0 = 8.5 \times 10^{-5}$ M). The inset is the TEM image of the synthesized hybrid microrattle with a gold nanocore (18 nm in diameter) and PEG brushes (M_n = 5000 g/mol) on the exterior surfaces. The reduction kinetics were monitored by time-dependent changes in UV−vis absorption spectra of the *p*-nitrophenol reactant in the reaction mixture (Figure S10, Supporting Information).

were obtained after selective HF etching of the silica inner shell from the Ag@SiO_2@P(MAA-*co*-DVB)-*click*-PNIPAM microspheres. The FESEM and TEM images of the synthesized hairy Ag@air@P(MAA-*co*-DVB)-*click*-PNIPAM hybrid microrattles are shown in parts e and f of Figure 1, respectively. The silver nanocore encapsulated in the hollow cavity of the microsphere appears as bright spots in the FESEM micrograph when imaged at a high voltage of 15 kV. Well-defined rattle-type hybrid hollow structures are discernible from the TEM images of Figure 1f.

Polymer based nanoreactor systems have recently been explored for living radical polymerization and organic reactions.[49,50] One of the advantages of synthesizing hairy hybrid microrattles with the exterior surface decorated by hydrophilic PEG brushes is their enhanced dispersity in an aqueous medium. The present hairy Au@air@P(MAA-*co*-DVB)-*click*-PEG hybrid microrattles were employed as a nanoreactor system for the well-established reduction of *p*-nitrophenol to *p*-aminophenol to illustrate their potential applications. Hairy Au@air@P(MAA-*co*-DVB)-*click*-PEG hybrid microrattles were initially dispersed in an aqueous medium upon brief sonication, followed by equilibrating in the $NaBH_4$ solution (0.6 M) for 30 min at room temperature (25 °C). Upon addition of *p*-nitrophenol into the mixture, catalytic reduction was initiated by the Au NP in the confined space.[51,52] Figure 3 shows the catalytic reduction of *p*-nitrophenol in the cavity of Au@air@P(MAA-*co*-DVB)-*click*-PEG hybrid microrattles (1.9×10^{-6} M). The inset is the TEM image of the synthesized hybrid microrattle with a gold nanocore (18 nm in diameter) and PEG brushes (M_n = 5000 g/mol) on the exterior surfaces. The reduction kinetics were monitored by time-dependent changes in UV−vis absorption spectra of the *p*-nitrophenol reactant in the reaction mixture (Figure S10, Supporting Information). As the catalytic reaction proceeds, the characteristic absorption peak of the reactant (*p*-nitrophenol) at 400 nm decreases with a concomitant increase in the absorption peak of the product (*p*-aminophenol) at 295−300 nm.[51−54] During the catalytic reaction process, *p*-nitrophenol first diffused through the polymer shell into the hollow cavity. The catalytic reduction was then initiated by electron transfer from the donor BH_4^- to the substrate *p*-nitrophenolate ion on the Au NP surface.[52] Finally, the *p*-aminophenol product desorbed from the gold NP surfaces. No catalytic reduction of *p*-nitrophenol was observed in the absence of Au@air@P(MAA-*co*-DVB)-*click*-PEG hybrid microrattles. Thus, the synthesized hairy hybrid microrattles can serve as a spatially confined nanoreactor system for catalytic reactions.

CONCLUSIONS

Bifunctional hairy metal@air@polymer hybrid microrattles, with a catalytic metal nanocore (Au or Ag) in the cavity and functional polymer brushes (PEG or PNIPAM) on the exterior surface, have been synthesized from the hairy Au@SiO_2@P(MAA-*co*-DVB)-*click*-PEG and Ag@SiO_2@P(MAA-*co*-DVB)-*click*-PNIPAM core−double shell microspheres by etching of the silica inner layer. The so-obtained hollow microspheres exhibited well-defined rattle-type morphology and tailored surface functions. The bifunctional hybrid microrattles were finally applied as a nanoreactor system for the confined catalytic reduction of *p*-nitrophenol. Combined interior functionalization and exterior modification of the hollow polymer microspheres with a catalytic metal nanocore and functional polymer brushes, respectively, provides a general approach for endowing the hollow polymer microspheres with unique morphology and functions, leading to useful multifunctional hollow polymer nano- and microstructures.

ASSOCIATED CONTENT

Supporting Information. Experimental section, TEM images of the gold and Ag NPs, Ag@SiO_2-MPS and Ag@SiO_2@P(MAA-*co*-DVB) microspheres, FT-IR spectra of the Au@SiO_2-MPS, Au@SiO_2@P(MAA-*co*-DVB), Au@SiO_2@P(MAA-*co*-DVB)-*click*-PEG, Ag@SiO_2@P(MAA-*co*-DVB), and Ag@SiO_2-@P(MAA-*co*-DVB)-*click*-PNIPAM microspheres, XPS S 2p core-level spectrum of the PEG-SH chains, XPS and DLS analyses of the Ag@SiO_2@P(MAA-*co*-DVB)-*click*-PNIPAM hairy core−double shell microspheres, UV−vis absorption spectra of the catalytic reaction mixtures. This material is available free of charge via the Internet at http://pubs.acs.org.

AUTHOR INFORMATION

Corresponding Author

*E-mail: cheket@nus.edu.sg; Tel (65) 65162189; Fax (65) 67791936.

REFERENCES

(1) Wang, Y.; Hu, H. P.; Zhang, X. *Adv. Mater.* **2009**, *21*, 2849–2864.
(2) Lou, X. W.; Archer, L. A.; Yang, Z. C. *Adv. Mater.* **2008**, *20*, 3987–4019.
(3) Fu, G. D.; Li, G. L.; Neoh, K. G.; Kang, E. T. *Prog. Polym. Sci.* **2011**, *36*, 127–167.
(4) De Koker, S.; De Geest, B. G.; Cuvelier, C.; Ferdinande, L.; Deckers, W.; Hennink, W. E.; De Smedt, S.; Mertens, N. *Adv. Funct. Mater.* **2007**, *17*, 3754–3763.
(5) Piao, Y.; Burns, A.; Kim, J.; Wiesner, U.; Hyeon, T. *Adv. Funct. Mater.* **2008**, *18*, 3745–3758.
(6) Arnal, P. M.; Comotti, M.; Schüth, F. *Angew. Chem., Int. Ed.* **2006**, *45*, 8224–8227.

(7) Xie, L.; Zheng, J.; Liu, Y.; Li, Y.; Li, X. G. *Chem. Mater.* **2008**, *20*, 282–286.
(8) Wang, L.; Tang, F.; Ozawa, K.; Chen, Z. G.; Mukherj, A.; Zhu, Y.; Zou, J.; Cheng, H. M.; Lu, G. Q. *Angew. Chem., Int. Ed.* **2009**, *48*, 7048–7051.
(9) Xu, X. L.; Asher, S. A. *J. Am. Chem. Soc.* **2004**, *126*, 7940–7945.
(10) Li, G. L.; Kang, E. T.; Neoh, K. G.; Yang, X. *Langmuir* **2009**, *25*, 4361–4364.
(11) Chen, D. Y.; Jiang, M. *Acc. Chem. Res.* **2005**, *38*, 494–502.
(12) Li, G. L.; Liu, G.; Kang, E. T.; Neoh, K. G.; Yang, X. *Langmuir* **2008**, *24*, 9050–9055.
(13) Boyer, C.; Whittaker, M. R.; Nouvel, C.; Davis, T. P. *Macromolecules* **2010**, *43*, 1792–1799.
(14) Liu, X.; Basu, A. *J. Am. Chem. Soc.* **2009**, *131*, 5718–5719.
(15) Kamata, K.; Lu, Y.; Xia, Y. *J. Am. Chem. Soc.* **2003**, *125*, 2384–2385.
(16) Li, G. L.; Yang, X. L. *J. Phys. Chem. B* **2007**, *111*, 12781–12786.
(17) Liu, G. Y.; Ji, H. F.; Yang, X. L.; Wang, Y. M. *Langmuir* **2008**, *24*, 1019–1025.
(18) Yin, Y.; Rious, R. M.; Erdonmez, C. K.; Hughes, S. G.; Somorjai, A.; Alivisatos, A. P. *Science* **2004**, *282*, 711–714.
(19) Arnal, P. M.; Comotti, M.; Schüth *Angew. Chem., Int. Ed.* **2006**, *45*, 8224–8227.
(20) Khalavka, Y.; Becker, J.; Sönnichsen, C. *J. Am. Chem. Soc.* **2009**, *131*, 1871–1875.
(21) Gao, J.; Liang, G.; Cheung, J. S.; Pan, Y.; Kuang, Y.; Zhao, F.; Zhang, B.; Zhang, X.; Wu, E. X.; Xu, B. *J. Am. Chem. Soc.* **2008**, *130*, 11828–11833.
(22) Hoyle, C. E.; Bowman, C. N. *Angew. Chem., Int. Ed.* **2010**, *49*, 1540–1573.
(23) Hoyle, C. E.; Lowe, A. B.; Bowman, C. N. *Chem. Soc. Rev.* **2010**, *39*, 1355–1387.
(24) DeForest, C. A.; Polizzotti, B. D.; Anseth, K. S. *Nature Mater.* **2009**, *8*, 659–664.
(25) Franc, G.; Kakkar, A. K. *Chem. Soc. Rev.* **2010**, *39*, 1536–1544.
(26) Lowe, A. B. *Polym. Chem.* **2010**, *1*, 17–36.
(27) van Berkel, K. Y.; Hawker, C. J. *J. Polym. Sci., Part A: Polym. Chem.* **2010**, *48*, 1594–1606.
(28) Li, G. L.; Wan, D.; Neoh, K. G.; Kang, E. T. *Macromolecules* **2010**, *43*, 10275–10282.
(29) Goldmann, A. S.; Walther, A. W.; Nebhani, L.; Joso, R.; Ernst, D. E.; Loos, K.; Barner-Kowollik, C.; Barner, L.; Müller, A. H. E. *Macromolecules* **2009**, *42*, 3707–3714.
(30) Wickard, T. D.; Nelsen, E.; Madaan, N.; Brummelhuis, N.; Diehl, C.; Schlaad, H.; Davis, R. C.; Linford *Langmuir* **2010**, *26*, 1923–1928.
(31) van der Ende, A. E.; Harrell, J.; Sathiyakumar, V.; Meschievitz, M.; Katz, J.; Adcock, K.; Harth, E. *Macromolecules* **2010**, *43*, 5665–5671.
(32) van der Ende, A.; Croce, T.; Hamilton, S.; Sathiyakumar, V.; Harth, E. *Soft Matter* **2009**, *5*, 1417–1425.
(33) Weinrich, D.; Köhn, M.; Jonkheijm, P.; Westerlind, U.; Dehmelt, L.; Engelkamp, H.; Christianen, P. C. M.; Kuhlmann, J.; Maan, J. C.; Nüsse, D.; Schröder, H.; Wacker, R.; Voges, E.; Breinbauer, R.; Kunz, H.; Niemeer, C. M.; Waldmann, H. *ChemBioChem* **2010**, *11*, 235–247.
(34) Weinrich, D.; Lin, P. C.; Jonkheijm, P.; Nguyen, U.; Schroder, H.; Niemeyer, C. M.; Alexandrov, K.; Goody, R.; Waldmann, H. *Angew. Chem., Int. Ed.* **2010**, *49*, 1252–1257.
(35) Stöber, W.; Fink, A.; Bohn, E. *J. Colloid Interface Sci.* **1968**, *26*, 62–69.
(36) Bourgeat-Lami, E.; Lang, J. *J. Colloid Interface Sci.* **1998**, *197*, 293–308.
(37) Li, G. L.; Xu, L. Q.; Tang, X. Z.; Neoh, K. G.; Kang, E. T. *Macromolecules* **2010**, *43*, 5797–5803.
(38) Gaborieau, M.; Nebhani, L.; Graf, R.; Barner, L.; Barner-Kowollik, C. *Macromolecules* **2010**, *43*, 3868–3875.
(39) Li, G. L.; Shi, Q.; Yuan, S. J.; Kang, E. T.; Neoh, K. G.; Yang, X. *Chem. Mater.* **2010**, *22*, 1309–1317.
(40) Barner, L. *Adv. Mater.* **2009**, *21*, 2547–2553.
(41) Waku, T.; Matsusaki, M.; Kaneko, T.; Akashi, M. *Macromolecules* **2007**, *40*, 6385–6392.
(42) Shi, D. J.; Matsusaki, M.; Akashi, M. *Bioconjugate Chem.* **2009**, *20*, 1917–1923.
(43) Wattendorf, U.; Kreft, O.; Textor, M.; Sukhorukov, G. B.; Merkle, H. P. *Biomacromolecules* **2008**, *9*, 100–108.
(44) Moulder, J. F.; Stickle, W. F.; Sobol, P. E.; Bomben, K. D. In *X-ray Photoelectron Spectroscopy*; Chastain, J., Ed.; Perkin-Elmer: Eden Prairie, MN, 1992.
(45) Li, G. L.; Zeng, D. L.; Wang, L.; Zong, B. Y.; Neoh, K. G.; Kang, E. T. *Macromolecules* **2009**, *42*, 8561–8565.
(46) Guerrero-Martínez, A.; Pérez-Juste, J.; Liz-Marzán, L. M. *Adv. Mater.* **2010**, *22*, 1182–1195.
(47) Schilli, C. M.; Zhang, M. F.; Rizzardo, E.; Thang, S. H.; Chong, Y. K.; Edwards, K.; Karlsson, G.; Müller, A. H. E. *Macromolecules* **2004**, *37*, 1159–1168.
(48) Wu, C.; Zhou, S. Q. *Macromolecules* **1995**, *28*, 5388–5390.
(49) Monteiro, M. J. *Macromolecules* **2010**, *43*, 1159–1168.
(50) Urbani, C. N.; Monteiro, M. J. *Macromolecules* **2009**, *42*, 3884–3886.
(51) Huang, X. Q.; Guo, C. Y.; Zuo, J. Q.; Zheng, N. F.; Stucky, G. D. *Small* **2009**, *5*, 361–365.
(52) Lee, J.; Park, J, C.; Song, H. *Adv. Mater.* **2008**, *20*, 1523–1528.
(53) Kuroda, K.; Ishida, T.; Haruta, M. *J. Mol. Catal. A: Chem.* **2009**, *298*, 7–11.
(54) Zhang, Q.; Zhang, T. R.; Ge, J. P.; Yin, Y. D. *Nano Lett.* **2008**, *8*, 2867–2871.